



Designation: D8093 – 19

Standard Guide for Nondestructive Evaluation of Nuclear Grade Graphite¹

This standard is issued under the fixed designation D8093; the number immediately following the designation indicates the year of original adoption or, in the case of revision, the year of last revision. A number in parentheses indicates the year of last reapproval. A superscript epsilon (ϵ) indicates an editorial change since the last revision or reapproval.

1. Scope*

1.1 This guide provides general tutorial information regarding the application of conventional nondestructive evaluation technologies (NDE) to nuclear grade graphite. An introduction will be provided to the characteristics of graphite that defines the inspection technologies that can be applied and the limitations imposed by the microstructure. This guide does not provide specific techniques or acceptance criteria for end-user examinations but is intended to provide information that will assist in identifying and developing suitable approaches.

1.2 The values stated in SI units are to be regarded as the standard.

1.2.1 *Exception*—Alternative units provided in parentheses are for information only.

1.3 *This standard does not purport to address all of the safety concerns, if any, associated with its use. It is the responsibility of the user of this standard to establish appropriate safety, health, and environmental practices and determine the applicability of regulatory limitations prior to use.*

1.4 *This international standard was developed in accordance with internationally recognized principles on standardization established in the Decision on Principles for the Development of International Standards, Guides and Recommendations issued by the World Trade Organization Technical Barriers to Trade (TBT) Committee.*

2. Referenced Documents

2.1 *ASTM Standards:*²

[D7219 Specification for Isotropic and Near-isotropic Nuclear Graphites](#)

[E94 Guide for Radiographic Examination Using Industrial Radiographic Film](#)

[E1025 Practice for Design, Manufacture, and Material](#)

¹ This guide is under the jurisdiction of ASTM Committee D02 on Petroleum Products, Liquid Fuels, and Lubricants and is the direct responsibility of Subcommittee D02.F0 on Manufactured Carbon and Graphite Products.

Current edition approved Nov. 1, 2019. Published December 2019. Originally approved in 2016. Last previous edition approved in 2016 as D8093 – 16. DOI: 10.1520/D8093-19.

² For referenced ASTM standards, visit the ASTM website, www.astm.org, or contact ASTM Customer Service at service@astm.org. For *Annual Book of ASTM Standards* volume information, refer to the standard's Document Summary page on the ASTM website.

[Grouping Classification of Hole-Type Image Quality Indicators \(IQI\) Used for Radiography](#)
[E1441 Guide for Computed Tomography \(CT\)](#)

3. Summary of Guide

3.1 This guide describes the impact specific material properties have on the application of three nondestructive evaluation technologies: Eddy current/electromagnetic testing (ET) (surface/near surface interrogation), ultrasonic testing (UT) (volumetric interrogation), radiographic (X-ray) testing (RT) (volumetric interrogation), to nuclear grade graphite.

4. Significance and Use

4.1 Nuclear grade graphite is a composite material made from petroleum or a coal-tar-based coke and a pitch binder. Manufacturing graphite is an iterative process of baking and pitch impregnation of a formed billet prior to final graphitization, which occurs at temperatures greater than 2500 °C. The impregnation and rebake step is repeated several times until the desired product density is obtained. Integral to this process is the use of isotropic cokes and a forming process (that is, isostatically molded, vibrationally molded, or extruded) that is intended to obtain an isotropic or near isotropic material. However, the source, size, and blend of the starting materials as well as the forming process of the green billet will impart unique material properties as well as variations within the final product. There will be density variations from the billet surface inward and different physical properties with and transverse to the grain direction. Material variations are expected within individual billets as well as billet-to-billet and lot-to-lot. Other manufacturing defects of interest include large pores, inclusions, and cracks. In addition to the material variation inherent to the manufacturing process, graphite will experience changes in volume, mechanical strength, and thermal properties while in service in a nuclear reactor along with the possibility of cracking due to stress and oxidation resulting from constituents in the gas coolant or oxygen ingress. Therefore, there is the recognized need to be able to nondestructively characterize a variety of material attributes such as uniformity, isotropy, and porosity distributions as a means to assure consistent stock material. This need also includes the ability to detect isolated defects such as cracks, large pores and inclusions, or distributed material damage such as material loss due to oxidation. The use of this guide is to acquire a basic

*A Summary of Changes section appears at the end of this standard

understanding of the unique attributes of nuclear grade graphite and its application that either permits or hinders the use of conventional eddy current, ultrasonic, or X-ray inspection technologies.

5. Graphite Properties

5.1 **Table 1** provides a summary of pertinent material properties for a limited selection of commercial nuclear graphite types.

5.2 The composite nature of graphite results in a multipart microstructure with variably shaped and sized porosity (see **Fig. 1**). The innate porosity in essence forms a flaw population that, in part, dictates not only material properties, but the minimum size limit of isolated flaws that conventional NDE technologies can and or should differentiate. However, this is not to overlook the potential need to detect and characterize distributed flaw populations such as oxidation or radiation damage that may be dimensionally smaller than the inherent porosity. The nature of the microstructure along with the material properties of low electrical conductivity, low acoustic velocity, and limited material constituents will dictate how the various NDE technologies can be applied and limit the information available from the examinations.

6. Eddy Current Examinations

6.1 Eddy current testing (ET) is an established inspection technology well suited for surface/near surface inspection of electrically conductive components. ET is based on generating eddy currents in an electrically conductive test sample through inductive coupling with a test coil. The characteristics and depth of the interrogating eddy currents are governed by the bulk electromagnetic properties of the test piece, test piece geometry, test frequency, and degree of electromagnetic coupling. The primary electromagnetic properties of interest are electrical conductivity and magnetic permeability. Any material or physical condition (for example, cracks, porosity, changes in grain structure, or different phases) that locally affects one or both of these properties can be detected and characterized. Typically, material anomalies are sensed through changes in the drive coil impedance when coupled to the test piece but can also be detected by means of secondary pickup induction coils or other magnetic field measurement technologies, for example, Hall or giant magnetoresistive

(GMR) devices. The approaches and test probes that can be implemented are diverse and dependent on the type, size, and location of the material anomaly or condition of interest as well as the test piece electromagnetic properties, geometry, surface condition, microstructure, temperature, and so forth.

6.2 Eddy currents can be used to inspect nuclear graphite for the presence of surface/near surface cracks, voids, and inclusions as well as to characterize the distribution of porosity or other distributed flaw populations that affect the bulk electrical conductivity. Aspects to consider when applying eddy currents to nuclear graphite include its low electrical conductivity, microstructure, and test conditions. The measured electrical conductivity of nuclear graphite is in the range of 0.1×10^6 S/m to 0.9×10^6 S/m, making it less than or nearly equal in conductivity to low conductivity metal alloys such as Ti-6Al-4V titanium (0.58×10^6 S/m), Inconel 600 (1.02×10^6 S/m), and stainless steel 304 (1.39×10^6 S/m) **(1)**.³ For low conductivity materials such as this, the dominance of the skin effect (the exponential decay of eddy current density in test sample) will be significantly reduced compared to that of the probe coil diameter to control depth sensitivity. The plane-wave approximation of eddy current density, j_x , in a test piece yields **Eq 1 (2)**:

$$j_x = j_0 e^{-x \sqrt{(\pi f \mu \sigma)}} \tag{1}$$

where:

- j_x = current density in test piece at depth x (A/m²),
- j_0 = current density at test piece surface (A/m²),
- x = depth into test piece (m),
- π = 3.1416,
- f = test frequency (Hz),
- μ = magnetic permeability in free space ($4\pi \times 10^{-7}$ H/m), and
- σ = test piece electrical conductivity (S/m).

6.3 The standard depth of penetration, $\delta = 1/\sqrt{(\pi f \mu \sigma)}$, is defined as the depth at which the eddy current density drops to 1/e or 36.8 % of the value of j_0 . Although eddy currents will be generated past 1δ , they attenuate rapidly. Eddy current density at 2δ is only 13.5 % of j_0 . It should also be noted that the phase

³ The boldface numbers in parentheses refer to a list of references at the end of this standard.

TABLE 1 Graphite Properties^A

Graphite Designation/Manufacturer	Density (kg/m ³)		Electrical Resistivity (μΩ·m)		L-Wave Acoustic Velocity (km/s)		S-Wave Acoustic Velocity (km/s)		Maximum Average Particle (Grain) Size (mm)	Forming Process
	WG	AG	WG	AG	WG	AG	WG	AG		
PCEA/ GrafTech International	1.775e+003	1.781e+003	7.49	8.01	2.65	2.56	1.59	1.58	0.7	Extruded
NBG-17/ SGL Group	1.850e+003	1.843e+003	9.51	9.84	2.77	2.76	1.61	1.61	0.8	Vibrationally molded
NBG-18/ SGL Group	1.871e+003	1.872e+003	9.57	9.16	2.87	2.93	1.67	1.68	1.6	Vibrationally molded
IG-110/ Toyo Tanso USA Inc.	1.777e+003	1.778e+003	11.24	10.98	2.46	2.51	1.56	1.57	0.01	Isostatically molded
IG-430/ Toyo Tanso USA Inc.	1.812e+003	1.814e+003	9.78	8.62	2.40	2.57	1.54	1.58	0.01	Isostatically molded

^A Idaho National Laboratory AGC 2 sample measurements: Average values for small, evenly distributed samples sectioned from a single billet, against grain (AG) and with grain (WG) directions are determined by orientation of the primary sample axis when sectioned from billet.

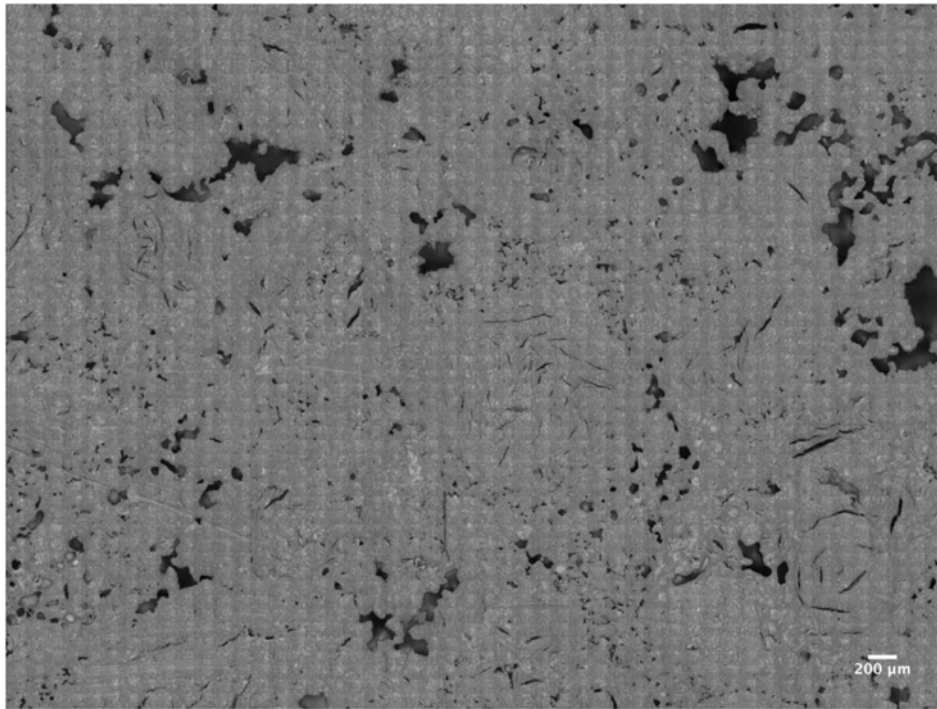


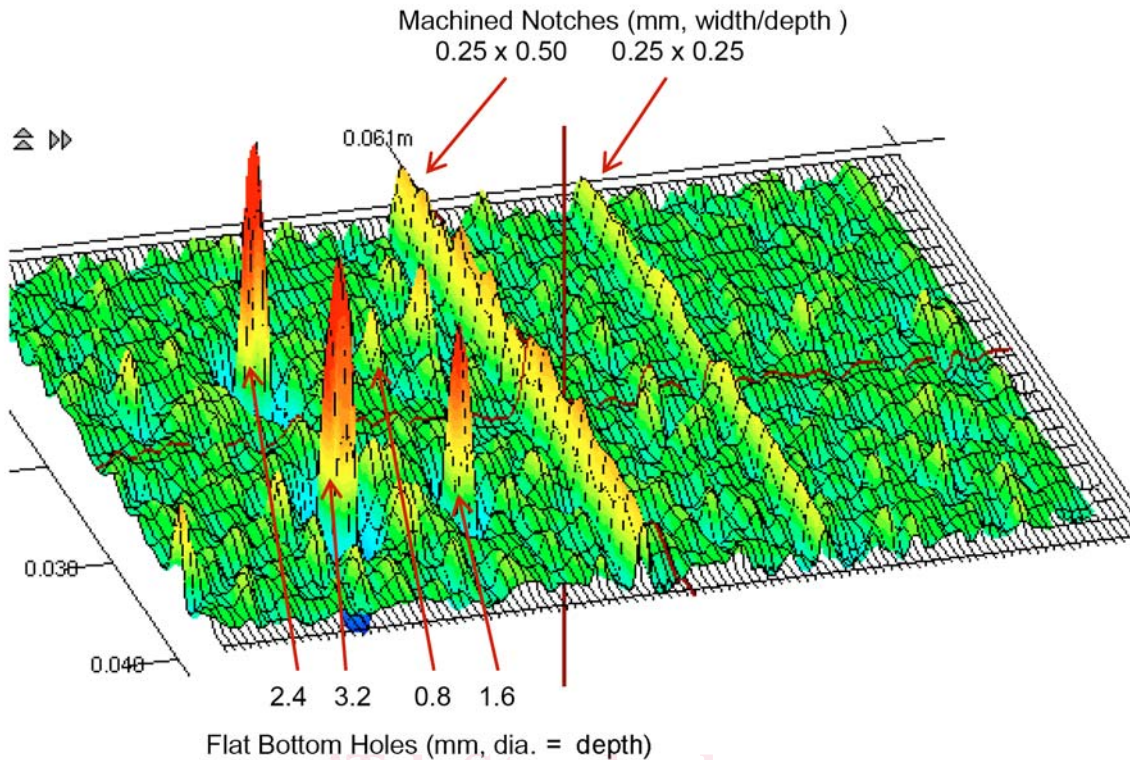
FIG. 1 Micrograph of SGL Group, NBG-18 Graphite

of the eddy currents progressively lags with depth into the test piece which is used to differentiate the source of the signal. Each standard depth produces 1 radian (57.3°) of phase lag. High current density yields good detectability and the standard depth of penetration is typically adjusted by means of manipulation of the test frequency to optimize current density and signal phase for defect detection or the measurement of interest. For example, selecting a test frequency that yields a δ at the depth where defects are expected to be located for a specific test piece should provide sufficient current density (approximately 37 % of surface current density) to detect defects at that depth and provide an approximate defect signal phase shift of 115° compared to a surface lift-off response (2). Lift-off is the response obtained from decoupling of the probe coil from the test piece due to increased probe-coil-to-test-piece separation or surface roughness, and higher test frequencies are required to get an equivalent δ for graphite compared to a metal. To get a $\delta = 0.005$ m in SS304 ($\sigma = 1.39 \times 10^6$ S/m), a test frequency of approximately 7.3 kHz is required. For graphite with a conductivity of 0.5×10^6 S/m, a test frequency of approximately 20.3 kHz is required. However, to obtain adequate eddy current density at the calculated skin depth, the induction probe coil must be able to project a sufficiently strong magnetic field to that depth.

6.4 A factor determining depth of penetration of the magnetic field into the test piece and thus the production of eddy currents will be the extent and magnitude of the axial field projected by a probe coil. The extent of the axial field projection is directly proportional to the diameter of the coil windings with a magnitude that decreases rapidly down the axis away from the coil. At an axial distance equal to $\frac{1}{3}$ the coil diameter the field strength is approximately 50 % of the field

strength at the coil face, and at a distance equal to 1 diameter only 10 % of the field strength remains (2). Compared to high conductivity metals, the projection limit of the axial field of the test coil may control the depth sensitivity in graphite versus skin depth. Therefore, proper selection of probe coil size combined with suitable low test frequencies will permit much thicker sections of graphite to be interrogated compared to an equivalent probe coil and a high conductivity metal combination. This provides the capability to perform limited volumetric examinations to detect large internal defects or characterize variations in bulk microstructural features such as porosity. Note that the area interrogated by the probe coil is proportional to its size and orientation. To improve detection of smaller surface defects, that is, concentrate eddy currents near the surface in a confined space, high test frequencies and smaller probe coils should be implemented (see Fig. 2). However, the coarse microstructure of some graphite types may introduce significant material noise. In this case, the 0.8 mm diameter by 0.8 mm deep flat bottom hole is equivalent in size to surface breaking porosity inherent to the graphite.

6.5 Per Specification D7219, grain sizes of the starting material in the mix for nuclear graphite can range from a maximum of 1.68 mm (medium grained) down to less than 2 micron (microfine grained). The size of the resulting microstructural features within the graphite (“grains” and porosity) will also range in a similar manner, as will the material noise recorded during inspections. That will limit the size of an anomaly or material variation that can be detected to something larger than the inherent microstructure. Medium grain materials will produce significantly more material noise than a fine grain material (see Fig. 3). This is especially true for the examination of machined surfaces using smaller diameter



The data was collected at 500 kHz using a 64 element transmit-receive array probe (2.0 mm coils separated by 2.5 mm, array element pitch is 1.25 mm). Although detectable, the 0.8 mm diameter by 0.8 mm deep flat bottom hole produces signals equivalent to the surface breaking porosity inherent to the graphite.

FIG. 2 Eddy Current Scan of NBG-18 Graphite Containing Artificial Flaws

probes at high test frequencies. The rough, as-manufactured surface of a billet will present a similar problem. The workmanship, finish, and appearance criteria in Specification D7219 only require a billet to be brushed clean after removal from the graphitization furnace resulting in rough, potentially uneven surfaces that will introduce significant material and lift-off noise into the signal. In both cases, probe diameter, design, test frequencies, or filtering can be adjusted to help mitigate the noise, assuming the defect or material anomaly of interest is of a nature to provide a relevant indication.

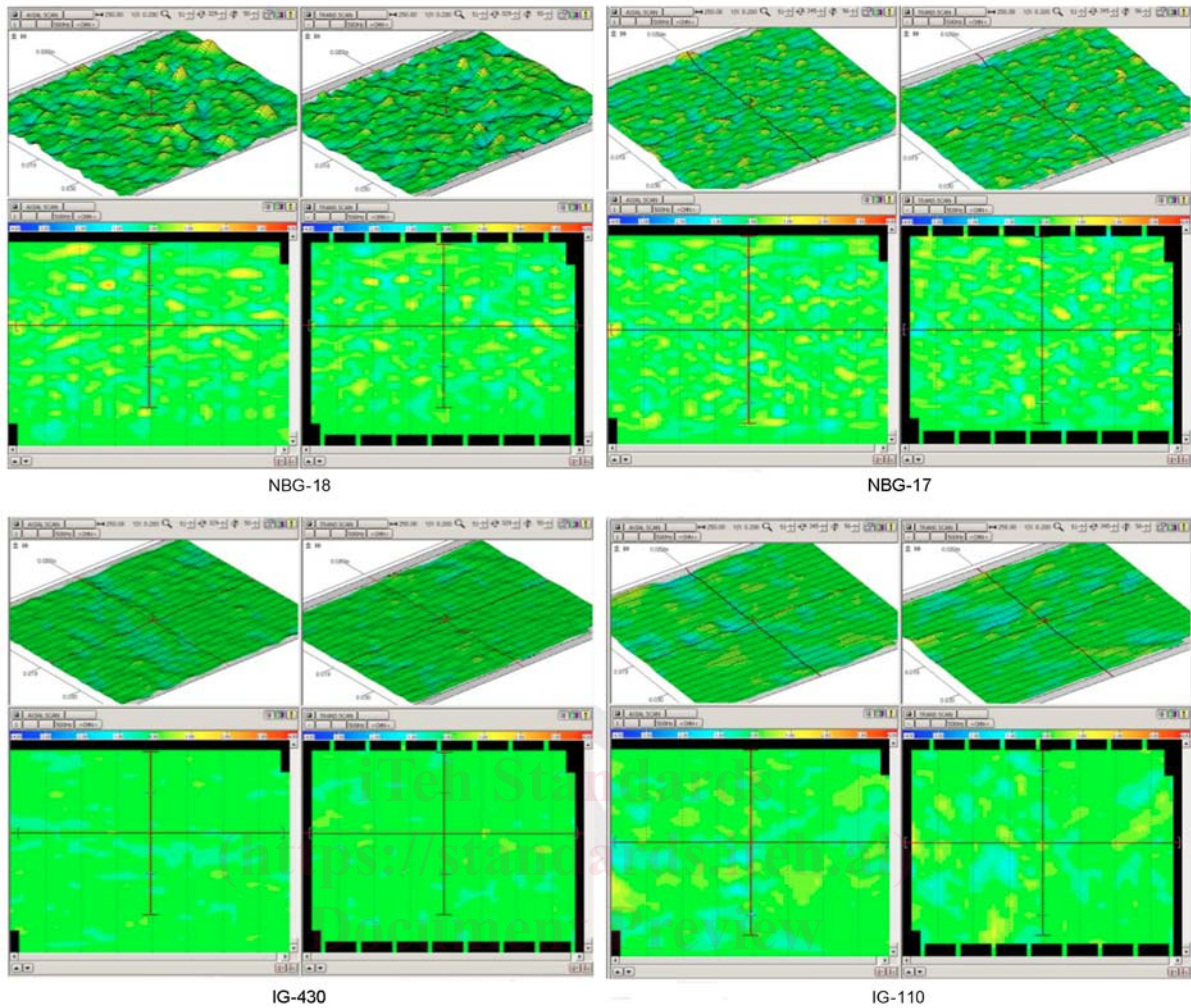
7. Ultrasonic Examinations

7.1 Ultrasonic inspection is based on the interaction of an acoustic wave with the material through which it is propagating. Isolated, macroscopic discontinuities are typically detected by means of their interaction with the acoustic wave to produce a reflection (echo) that propagates back to the transmitting transducer or a secondary pickup transducer. The nature of the interaction is defined, in part, by the mismatch of the acoustic impedance between the discontinuity and the matrix as well as the size of the discontinuity versus the ultrasonic wavelength. The acoustic impedance of a material is the product of its density and acoustic velocity and as the impedance mismatch at the boundary of a discontinuity increases, so does the amount of energy that is reflected.

7.1.1 Wavelength plays a role in that discontinuities equal to or larger than the wavelength will strongly interact with the passing wave, while those smaller than the acoustic wave-

length will have little interaction. As a result, test frequencies are typically selected to provide wavelengths smaller than the defects of interest. At a specific acoustic velocity, an increase in test frequency will decrease the wavelength size. However, the characteristic microstructure of graphite tends to strongly attenuate high test frequencies, reducing wave penetration into the graphite as well as limiting the size of defect that can be detected. An example of the high frequency attenuation that can be expected for a medium grain graphite is provided in Fig. 4. The transducer used for this example yielded a center frequency of 2.2 MHz for the first back wall reflection recorded from a 9.75 mm thick fused silica optical flat. Note that for the NBG-18, a test frequency of less than 1 MHz will be required to permit significant material penetration without excessive signal attenuation.

7.1.2 The acoustic velocity of NBG-18 is 2.9 km/s which yields a 5.8 mm wavelength at 0.5 MHz. As a rule of thumb, detection of isolated discontinuities with dimension of approximately one-half the ultrasonic wavelength is viable. Presented in Fig. 5 is a B-scan image from a 93.9 mm thick test block of NBG-18 graphite containing 3 mm diameter side-drilled holes ranging from 10 mm to 70 mm in depth from the surface. The B-scan data was collected using a 25.4 mm diameter, 0.5 MHz contact transducer with water coupling. The top and bottom surface of the test block were machined to provide uniform thickness and coupling. Note that a microstructural anomaly in the region of the 40 mm side-drilled hole significantly reduced



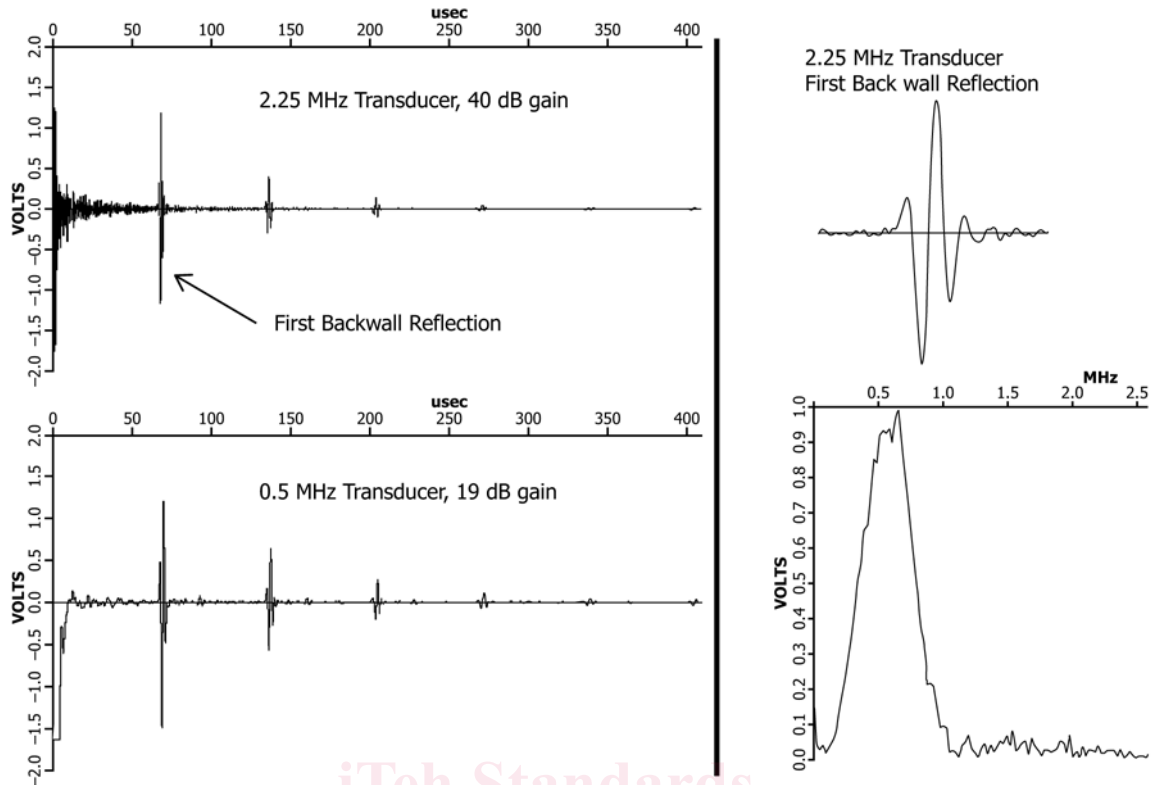
The approximate dimensions of each C-scan is 40 mm by 40 mm. The data was collected at 500 kHz using a 64 element transmit-receive array probe (2.0 mm coils separated by 2.5 mm, array element pitch is 1.25 mm). Two C-scans are obtained during a single scan. The transverse C-scan is primarily sensitive to transverse-oriented defects while the axial C-scan is sensitive to axial-oriented defects.

FIG. 3 Eddy Current C-Scans Comparing the Material Noise Obtained from Medium Grain (NBG-18, 1.6 mm and NBG-17, 0.8 mm Grain Size) Versus Superfine Grain (IG-430 and IG-110, 10 μ m Grain Size) Nuclear Graphites

the signal-to-noise ratio for this indication. Using instrumentation or techniques that increase the acoustic energy introduced into the material (such as high-energy narrowband techniques) will improve acoustic wave penetration and signal-to-noise ratios for material anomalies. Finer grain graphite will still exhibit significant attenuation. Overall, the intrinsic material variations often observed in graphite will reduce depth and sizing accuracy.

7.1.3 Fig. 6 compares ultrasonic back wall echoes from the 93.9 mm thick NBG-18 graphite (1.6 mm grain size) test block to those from an 88.8 mm thick IG-110 graphite (10 μ m grain size) test block. The A-scans were collected using the same instrument settings and the same 25.4 mm diameter, 2.25 MHz transducer used in Fig. 4. Although the superfine grain IG-110 graphite suffers less attenuation, the center frequency of the back wall reflection still drops to approximately 1 MHz (waveform and Fourier transform bottom of Fig. 6) from the 2.25 MHz center frequency of the input signal and has a highly attenuated second back wall reflection.

7.1.4 Ultrasonics can also be used to perform material characterization or detect distributed flaw populations by means of measurement of various wave propagation properties such as velocity, attenuation, or scattering. Elastic interactions as defined by the elastic constants influence acoustic velocity which can also be modified by acoustic energy scattered from the microstructure. Anelastic interactions result in loss of propagating wave energy by mechanisms that produce heat or transformation into different forms of sound. Of the three properties, velocity measurements will be the most viable approach to acquiring information regarding material uniformity (microstructure and porosity), isotropy, or the presence of distributed flaw populations. Fig. 7 compares time-of-flight C-scans from sections of machined NBG-17 and NBG-18 test blocks. The data were collected using a 25.4 mm, 0.5 MHz contact transducer with water couplant. The values presented are the round trip time-of-flight to the maximum negative peak amplitude of the back wall reflection. Neglecting possible variations in thickness due to tolerances in machining, the



A square wave pulser-receiver was used with 25.4 mm diameter, 2.25 MHz, and 0.5 MHz contact transducers with water couplant. Pulse width was set using fixed instrument settings, and no frequency filters were engaged. (a): Complete A-scans with multiple backwall reflections. (b): First backwall reflection using 2.25 MHz transducer and corresponding waveform Fourier transform. The 0.6 MHz center frequency of the reflection indicates significant attenuation of the high frequency content in the propagating wave.

FIG. 4 Ultrasonic Pulse-Echo A-Scans, Collected at One Location from a 93.9 mm Thick Machined NBG-18 Graphite Plate

0.406 m thick NBG-18 test block had a 5 μs range in time-of-flight values compared to 1 μs range of the 0.467 m thick NBG-17 test block. These ultrasonic scans illustrate that the variation in acoustic velocity provides a measure of the uniformity of the microstructure and therefore the uniformity of the mechanical properties within each test piece.

7.1.5 The prior examples all used contact transducers with water coupling. Requirements to prevent contamination of the graphite may prevent the use of liquid coupling. Alternative technologies include dry contact roller probes, laser-based generation and detection, air-coupled transducers, and electromagnetic-based transducers. However, compared to liquid-coupled piezoelectric transducers, the efficiencies of ultrasonic wave generation and detection in the test piece for these approaches are reduced. For comparison, the response for a 0.5 MHz liquid-coupled transducer to an equivalent simulated dry contact roller probe is provided in Fig. 8. Transducer and instrument settings were the same for the two measurements. Although demonstrated to be a viable approach to ultrasonic coupling into graphite, a significant reduction in signal amplitude and quality is observed for the simulated roller probe. The loss of signal amplitude and quality will reduce measurement reliability and defect detection capabilities.

Also note that a transmit-receive arrangement for a roller probe would help to remove the signal interference introduced by the probe structure and test piece front surface at the depth of the side-drilled hole.

7.2 Noncontacting laser-based, air-coupled, or electromagnetically coupled ultrasonic approaches will eliminate the potential for material contamination by means of surface contact. Combinations of the different approaches, for example, laser generation with EMAT detection, have also been investigated (3). Although applicable, these approaches also have limitations with respect to sensitivity and their application to graphite.

7.3 Air-coupled ultrasound has been utilized for material interrogation primarily to detect defects in low-impedance solids such as foams, plastics, and composite materials. The challenge in using air-coupled ultrasound for solid materials is the large impedance mismatch between the air and the material that results in low energy transmission into the material. A similar loss of energy will occur at the transducer-air interface without impedance matching. The reflection coefficient, R , for an acoustic wave at normal incidence is (4):

$$R_p = (Z_2 - Z_1) / (Z_2 + Z_1) \quad (2)$$